An overview of the tube fabric of Pomatoceros (Polychaeta, Serpulidae), illustrated by examples from the British Isles

An overview of the tube fabric of *Pomatoceros* (Polychaeta, Serpulidae), illustrated by examples from the British Isles

J.O. Buckman

Institute of Petroleum Engineering, Centre for Environmental Scanning Electron Microscopy (CESEM), Heriot-Watt University, Riccarton, Edinburgh, EH14 4AS, Scotland, United Kingdom.

e-mail: jim.buckman@pet.hw.ac.uk

Tel: +44 (0) 131 451 3188

Abstract

The calcareous tube of *Pomatoceros* is one of the most highly studied serpulid dwelling tube-structures. Despite this, there is a lack of consensus regarding the number and types of fabric within the tube structure, and the three-dimensional distribution of the fabrics about the tube. These are here described in *Pomatoceros triqueter* within the coastal waters of Britain, with lamello-fibrillar, irregularly oriented prismatic and spherulitic-prismatic fabrics noted as the major ultrastructural components. Fabrics are distributed along a chevron-shaped growth lamella structure, passing progressively from lamello-fibrillar fabric on the inner part of the tube, to irregularly oriented prismatic fabric along the outer part. This model can be adequately applied to all previous descriptions of the ultrastructure of *Pomatoceros*. All analysed samples comprise Mg-calcite, with typically 10-15 mol% $MgCO_3$.

Keywords

Chevron structure*;* irregularly oriented prismatic; lamello-fibrillar; *Pomatoceros triqueter*; spherulitic-prismatic; *Spirobranchus*.

1. Introduction

Pomatoceros Philippi, 1844, is a common extant serpulid that forms a calcareous-tube, which has a roughly 'triangular' cross-section, with an axial ridge developed along its upper surface. *Pomatoceros* has recently been assigned to *Spirobranchus* de Blainville, 1818, by a number of authors (Pillai, 2009; Vinn et al., 2009). However, material from the temperate waters of the North Atlantic, is still commonly assigned to *Pomatoceros*, and have been described historically as such by a number of authors (Bianchi, 1992; Campbell and Nicholls, 1994; Vinn and Zaton, 2012; Weedon, 1994). Here we follow ten Hove and Kupriyanova (2009), and retain *Pomatoceros*.

The tube of *Pomatoceros* has been described by a number of authors (Hedley, 1958; Vinn et al., 2009; Weedon, 1994), with Weedon (1994) and Vinn et al. (2009) detailing aspects of tube ultrastructure. Details concerning the presence and distribution of fabrics differ between the published papers and the current work. This paper aims to reconcile these anomalies, by unification under a new model based upon the present study. The tube structure of *Pomatoceros triqueter* (Linnaeus, 1758) is therefore described at a macro- to ultrastructural level, using a range of materials collected throughout the British Isles.

2. Material and methods

In excess of twenty-five individual samples were prepared and examined, from localities around the British Isles. This material can be assigned to *P. triqueter* based on the illustrations and description of Bianchi (1992).

Materials were analysed using an FEI Quanta 650 FEG ESEM, a Phillips XL30 LaB_6 ESEM and a Hitachi S-4100 FEG SEM.

Both natural and broken surfaces were examined, as well as samples impregnated in resin and examined as polished blocks or thin-sections. Some samples were treated with a 5% solution of bleach, or dilute (1.5%) HCl acid. Polished blocks and thin-sections were also examined using MAPS^{TM} an automated image acquisition and stitching programme (see Buckman, 2014).

Eight samples were analysed by powder X-Ray Diffraction (XRD). Energy Dispersive X-ray analysis (EDX), using an Oxford Instruments X-max^{N} 150 mm detector, was also utilised.

3. Results

The tube structure of *P. triqueter* can conveniently be considered at three levels: macro-, micro- and ultrastructural.

3.1. Macrostructure

Tubes typically in the region of 3 mm wide. Triangular in transverse section (Fig. 1A), with a well-developed axial ridge, which protrudes beyond the aperture (Fig. 1B). Mature specimens exhibit a thickening of the aperture to give the appearance of a collar (Fig. 1B). Encrusting surfaces, with base exhibiting a cellular alveolar structure (Fig. 1A), which are 200-500 µm in size, and vary in shape from irregular to lunate. A perforated tabulae ('grating') is occasionally observed towards the distal end of the tube (Fig. 1G). Specimens occur either individually, attached directly to a variety of substrates, or as tortuous masses of twisted individuals in knotted

'spherical' agglomerations. In some rare cases, a substantial section of the tube can be lifted up from the surface, although this is generally rare.

Pomatoceros triqueter has a calcified operculum, in the form of a convex disc or inverted cone, with variably developed tripartite horns at the apex (Fig. 1E, F).

3.2. Microstructure

The tube of *P. triqueter* comprises two types of layer, the chevron layer, and the pseudo-laminar layer (Fig. 1A, C, D, 2), of which the former is usually quantitatively the more important. The pseudo-laminar layer is the attenuated distal extension of the chevron layer, occurring on the outer surface of the tube. The boundary between the two is usually sharp and relatively straight, but may also be undulatory (Fig. 1C, D), typically having an unconformable angular relationship.

Both layers are composed of individual growth lamellae, which form either simple sheet-like structures, or lens–shaped pods and are clearly chevron-shaped with their apex directed towards the aperture (Fig. 1C, D, 2).

Organic membranes are commonly observed, especially in the chevron layer (Fig. 1C, D).

3.3. Ultrastructure

Three main styles of fabric can be recognised within the main tube: lamello-fibrillar, irregularly oriented prismatic, and spherulitic-prismatic. Additionally a lozenge fabric and a platey fabric occur but to a limited extent. Lamello-fibrillar and irregularly orientated prismatic fabrics represent the dominant style of ultrastructure.

3.3.1. Lamello-fibrillar fabric

Forming wedge or lens shaped lamellae that are typically 0.97 - 12.56 µm thick (average 4.63 µm, n = 61). Comprising individual lath-shaped elements that are oriented parallel or sub-parallel to each other, and occur at a low angle to, or parallel to, growth lamellae (Fig. 3A). Between successive lamella, laths are typically oriented in different directions, at up to 90˚ from laths in the previous lamella (Fig. 3A). Individual laths are 145 - 776 nm wide (average 381 nm, n = 315) by several microns in length.

3.3.2. Irregularly oriented prismatic fabric

Comprising lath-like structures, with dimensions of 152 - 725 nm wide (average 363 nm, n = 296) by several microns in length. Laths are arranged in a completely unordered chaotic fashion, which displays no preferred orientation with respect to growth lamellae (Fig. 3B). Laths are commonly loosely packed, with lamellae having a porous appearance. Fabric is massive in appearance, with occasional hint of lamellae in the range 2.34 - 24.40 µm (average 7.04 µm, n = 29).

3.3.3. Spherulitic-prismatic fabric

Fine needle-like crystallites in the order of 34 – 99 nm wide (average 54 nm, n=87) by 3.86 – 16.89 µm or more in length (average 10.79 µm, n =20), occurring in micron sized bundles (Fig. 3C). Crystallites approximately perpendicular to growth lamellae, and exhibit a fan-like morphology (Fig. 3C, D), botryoidal appearance on growth surfaces (Fig. 3G). Individual crystallites continuous across minor growth lamellae. Occurring in lamellae of about 1 to 5 µm thick, but also in lenses up to 30 - 50 µm thick.

3.3.4 Lozenge fabric

Lozenge shaped ‘crystals’ (Fig. 3G, H), with both ends tapering, 379 - 811 nm wide (average 679 nm, n = 27), by 1.160 - 2.494 µm long (average 2.379 µm, n = 27). The latter are observed along the skirt at the front of the tube, and occur above a thick organic lamella, from which they appear to originate (Fig. 3G). Substructure uncertain.

3.3.5. Platey fabric

The tabulae (Fig. 1G) comprise flat platy crystals, with well-formed crystal terminations. Crystals occur radially, but with no specific preferred direction of growth (Fig. 1H).

3.3.6. Organic membranes

Organic membranes are occasionally observed between and within inorganic lamellae (Fig. 3E) of all three of the major fabrics. The structure of the organic layers often appears homogeneous. However, on rare occasions they are observed to have a fibrous structure (Fig. 3F), or appear as a fine meshwork (Fig. 3D). The latter may be due to degradation. The base of an organic membrane is often gradational in nature, while the upper surface is generally sharp.

3.3.7. Variation in fabric distribution

The fabric of the chevron lamellae change from inner to outer margin, in a progressive and predictable fashion, which is herein termed ‘differentiated chevron structure’. Lamello-fibrillar fabric occurs along the inner surface, and irregularly

oriented prismatic along the outer, with the change occurring approximately at the apex of the chevron (Fig. 2). The change either takes the form of tapering lamellae comprising lamello-fibrillar fabric, or a gradual passage from lamello-fibrillar to irregularly oriented prismatic fabric along an individual lamella.

Spherulitic-prismatic fabric occurs along the inner margin of the tube, where it is interleaved with lamello-fibrillar fabric, and has a growth vector in an inwards direction (towards the lumen). This fabric also occurs as the infill to irregular shaped pods (within the pseudo-laminar and chevron layers), as well as a lining within the cavities of alveoli. Additionally the fabric is particularly common near the aperture of mature specimens.

3.3.8. Operculum fabric

Opercula horns are often hollow, and after treatment with bleach solution, the tips can often disappear. The dominant fabric within opercula is a fibrous texture, with a granular sub-structure (Fig. 4A), with fibres in the order of 500 nanometres in width. Fibres are generally arranged radially (including within the horns), starting at the outer surface and orientated inwards, although also seen to be oriented parallel to opercula outer surface (Fig. 4B). On both external and internal surfaces, bundles of fibres are often constrained within polygonal packages (Fig. 4C, D). A more granular texture is sporadically observed, with granules rounded and approximately 500 nanometres or less in size (Fig. 4E). Spheroidal structures (30 to 50 microns wide) are also noted to occasionally occur near the outer surface (Fig. 4F). The tripartite horns and outer part of opercula are often densely pervaded by sinuous hollow tubes that run parallel to the outer surface of the opercula (Fig. 4G). These tubes are lined by radial masses of acicular or blade-like crystals (Fig. 4H). The inner surface of the

opercula can be covered by low mounds, in the order of 5 to 50 microns in width (Fig. 4D).

3.4. Composition

3.4.1. Tube composition

The occurrence of Mg-calcite was indicated by EDX analysis. All eight samples analysed by powder XRD, gave d_{104} values of between 2.99 and 3.01, indicating a Mg-calcite composition, with between 10 and 15 mol% $MgCO_3$ (Table 1).

3.4.2. Operculum composition

Analysis by EDX indicates that opercula are composed of calcium carbonate. Small amounts of Mg (1.8 wt%) are observed from the outer surface of the opercula, between the tripartite horns, otherwise the majority of the opercula lack any Mg content, but posses significant amounts of Sr (0.2 wt%); suggesting that opercula are formed from aragonite.

4. Discussion

4.1. Structure and distribution of fabrics

The fabric distributions determined here differs in detail from that of previous workers (Vinn et al., 2009; Weedon, 1994). Weedon (1994) recognised an overall chevron-shaped structure to the tube of *P. triqueter,* which was composed of an ordered chevron fabric (= lamello-fibrillar fabric), and the localised occurrence of unordered chevron fabric (= irregularly oriented prismatic fabric) towards the outer margin of the tube, although not illustrating this within his three-dimensional model (Weedon, 1994: fig. 2). Although Weedon (1994) recorded spherulitic-prismatic

fabric within *Spirorbis*, it was not noted from *Pomatoceros*. Vinn et al. (2009) described two fabric types in *Pomatoceros americanus* Day, 1973; lamello-fibrillar structure on the inner margin, and irregularly oriented prismatic structure along the outer parts of the tube. No mention was made of a chevron structure, although Vinn had previously illustrated a chevron structure to the tube of *P. triqueter* (Vinn and Zaton, 2012: fig. 8). Vinn et al. (2009) did not note the presence of spherulitic prismatic fabric within *P. americanus*. In addition, Vinn et al. (2008: table 2) and Vinn (2013: table 1) indicate that *Spirobranchus / P. triqueter* (from Sweden) only has lamello-fibrillar fabric.

Given the present observations, and those of the above mentioned authors, it is clear that the tube structure of *Pomatoceros* should be thought of in terms of a series of stacked simple chevron–shaped growth lamellae, in which the distal extremities on the outer margin of the tube are occasionally greatly attenuated away from the aperture, giving the appearance of an outer tube parallel laminar layer (the pseudo-laminar layer) (see Fig. 1A, C, D, 2). Ultrastructurally, the inner tube margin comprises a lamello-fibrillar fabric (ordered chevron structure of Weedon, 1994), passing into irregularly oriented prismatic fabric (unordered chevron fabric of Weedon, 1994), at about the apex of each chevron (Fig. 2); forming a ‘differentiated chevron’ structure. Additionally, minor developments of spherulitic-prismatic fabric can be sporadically observed at a variety of locations (Fig. 2). Given the Swedish material of Vinn (2013), and the comments of Weedon (1994), it is likely that both irregularly oriented prismatic fabric and spherulitic-prismatic fabrics are variable in occurrence within *Pomatoceros*.

4.2 Comparison of opercula

The opercula of *Pomatoceros* is not often described, with a notable exception being that of Vinn and ten Hove (2011) describing the opercula of *Spirobranchus giganteus* (*Pomatoceros* belonging to *Spirobranchus* according to Pillai (2009) and Vinn et al. (2009)). The opercula of *Pomatoceros triqueter* differs from that of *S. giganteus* in a number of major points. Firstly, *P.triqueter* has simple tripartite horns (sometimes vestigial), as opposed to well-developed antler-like horns. Secondly, there is no sign of an outer layer of irregularly ordered prismatic (IOP) fabric within *P. triqueter*. Thirdly, *S. giganteus* exhibits a plethora of large pores (~10 micron wide), clearly observed on the outer surface, that pass vertically through the opercula. Whereas, *P. triqueter* has 5-10 micron diameter sinuous hollow tubes that are parallel to the opercula outer surface, and restricted to the outer layer. The fibrous fabric observed within *P. triqueter* bears some similarity to elements of the irregular spherulitic prismatic structure from the opercula of *S. giganteus*, as well as the regular spherulitic prismatic structure within the opercula of *Pyrogopolan ctenactis* (see Vinn and ten Hove, 2011: fig. 4). The polygonal packaging of fibres within *P. triqueter* in particularly resembles the regular spherulitic prismatic structure from *Pyrogopolan ctenactis* (see Vinn and ten Hove, 2011: fig. 1d-f, 2c,d), although no organic membrane was detected from the current study. Further investigation of the fibrous fabric within the opercula of *P. triqueter* is warranted, although beyond the scope of the present paper.

The disappearance of the tips of horns from opercula is of importance, as this suggests a high organic content and compares to the situation with the opercula horns of *Pyrogopolan ctenactis* (Vinn and ten Hove, 2011).

The fibrous fabric observed within the opercula of *P. triqueter* is similar in many respects to the sphrerulitic prismatic fabric observed within the co-associated tubes,

the main difference being its apparent aragonitic composition as opposed to the Mg-calcite found within the tube. The occurrence of a Mg-calcite precursor layer in the opercula is therefore extremely important, indicating that the form of calcite produced can be readily switched, having implications on the relationship between this fabric between opercula and tube. It is possible that the mechanisms / organs responsible for the formation of both are the same, which is worthy of future investigation.

4.3. Composition

The tubes of *P. triqueter* analysed herein are all Mg-calcite, with powder XRD d_{104} values indicating between 10-15 mole % $MgCO_3$ (Goldsmith & Graf, 1958: table 5; Hardy and Tucker, 1988; Zhang *et al.* 2010: fig. 6). No peaks for aragonite were observed from the tubes. Samples were also analysed by EDX to determine the presence or absence of strontium, as the latter element can be taken as a proxy for aragonite (Taylor et al., 2010); however, no strontium was observed, from EDX analysis of the tubes, suggesting that the samples analysed only comprised Mg-calcite. The composition of many described samples of *Pomatoceros* from the literature are typically not given. One French sample of *P. triqueter* (from Marseille) is described as comprising 31% aragonite and 12.5 mol% $MgCO_3$ (Bornhold and Milliman, 1973: table 1). Such differences may be a factor of temperature (see Bornhold and Milliman, 1973). The samples from the present study are consistent with the range of compositions previously recorded for *Pomatoceros*. The distribution of mol% $MgCO_3$ values (Table 1) appears to show a general correlation with geographical distribution (latitude), with a trend towards increasing mol% $MgCO_3$ with higher latitudes; suggesting a possible link with water temperature. However, the most northerly sample also has one result the same as the most southerly. The latter may be spurious, although it should be noted that *Pomatoceros*

recorded from Marseille does not fit this trend either (Bornhold and Milliman, 1973: table 1). No specific data regarding water temperature, or other factors such as water depth were collected, therefore water temperature (latitude) may not be the main controlling factor for composition. This agrees with recent work, suggesting that serpulid tube composition may be controlled phylogenetically rather than by temperature (see Smith et al., 2013).

The aragonitic composition of the opercula is of interest, as it substantiates the ability of *Pomatoceros* to utilize aragonite during biomineralization, indicating that this is not just restricted to examples from warmer waters such as the Mediterranean Sea (see Bornhold and Milliman, 1973). The apparent lack of aragonite from the tube and the virtual 100% composition from the opercula requires further study, to elucidate the mechanism and origin of these differences.

4.4. Importance of organic layers

Vinn (2013) discussed the presence and significance of organic layers within serpulid genera, including *Spirobranchus triqueter* (= *P. triqueter*), where organic membranes were commonly associated with lamello-fibrillar fabric. The organic layers herein associated with lamello-fibrillar fabric appear to gradually form towards the end of deposition of a lamella, and form a sharp base for the next; they do, however, not terminate every lamella. This supports the findings of Vinn (2013). In the case of spherulitic-prismatic fabric, growth can be initiated along an organic membrane (Fig. 3D), with the membrane having a potential controlling role in the initialisation of mineral deposition. A close relationship is also suggested by the association of membraneous organic material within spherulitic-prismatic fabric. With irregularly oriented prismatic fabric, the relationship with organic material appears simpler,

forming a bulking agent for the randomly oriented lath like crystals. Analysis of the amino acid composition of such organic membranes would likely prove of interest in determining the relationship between organic membranes and calcite crystals.

5. Conclusions

P. triqueter has an interesting tube ultrastructure comprising lamello-fibrillar and irregularly oriented prismatic fabrics distributed across chevron-shaped lamellae. Lamello-fibrillar fabric occurs along the inner tube margin, changing to irregularly oriented prismatic fabric from about the inflection of the chevron. Irregularly oriented prismatic fabric on the outer surface can become greatly attenuated distally, developing a 'pseudo-laminar' layer. In addition, variable amounts of spherulitic-prismatic fabric can occur throughout the tube of *P. triqueter*, although this is not generally significantly developed. This pattern in ultrastructure distribution is typical of *Pomatoceros* in general, although all elements may not always be developed to such an extent. In the case of some *P. triqueter* tubes, ultrastructure may be restricted to lamello-fibrillar fabric (see Vinn, 2013).

The tube of *Pomatoceros* can vary from Mg-calcite to aragonite, although in the present study all samples were 100% Mg-calcite, and typically ranged between 10 – 15 mol% $MgCO_3$.

The nature and distribution of organic lamellae within *P. triqueter* agree with the findings of previous authors (Vinn, 2013).

The opercula are predominantly aragonite, with a fabric similar to irregular spherulitic prismatic and regular spherulitic prismatic structures within the opercula of other

annelids (see Vinn and ten Hove, 2011). Further study is likely to yield data of taxonomic significance.

The current work demonstrates the value of automated image collection and stitching software, such as 'MAPS', as it allows for high-resolution study of fabrics continuously over large areas, helping to clarify the nature of fabric distribution across the whole tube.

Acknowledgements

Many thanks to D. Harries (Heriot-Watt University, School of Life Sciences), and J.A. Todd (Natural History Museum, London) for some of the materials used during this study, and to M.J. Weedon for an introduction to serpulid tubes. G. Rosair (Heriot-Watt University, School of Engineering and Physical Sciences) and A. Forrester (University of the West of Scotland) provided XRD analysis. This manuscript has also benefited from review comments by P.D. Taylor (Natural History Museum, London). This paper is dedicated to the memory of Margaret Corrigan (University of the West of Scotland).

References

Bianchi, C.N. 1992. *Pomatoceros lamarkii* (Polychaeta: Serpulidae) in south-west Cornwall, with further notes on the distinction of the species of *Pomatoceros*. Porcupine Newsletter. 5, 127-130.

Blainville, H., de. 1818. Mémoire sur la classe des Sétipodes, partie des Vers à sang rouge de M. Cuvier, et des Annélides de M. de Lamarck. Bulletin de la Société Philomatique de Paris. 3, 78-85.

Bornhold, B.D., Milliman, J.D. 1973. Generic and environmental control of carbonate mineralogy in serpulid (Polychaete) tubes. Journal of Geology. 81, 363-373.

Buckman, J. 2014. Use of Automated Image Acquisition and Stitching by Scanning Electron Microscopy: Imaging of Large Scale Areas at High Resolution. Microscopy and Analysis. 28 (1), S13-15.

Campbell, A.C., Nicholls, J. 1994. Seashores and shallow seas of Britain and Europe. Hong Kong, Hamlyn, 320 pp.

Day, J.H. 1973. New Polychaeta from Beaufort, with a key to all species recorded from North Carolina. National Oceanic and Atmospheric Administation Technical Report, National Marine Fisheries Service, Circular. 375, 1-140.

Goldsmith, J.R., Graf DL. 1958. Relation between lattice constants and composition of the Ca-Mg carbonates. The American Mineralogist. 43, 84-101.

Hardy, R., Tucker, M. 1988. X-ray powder diffraction of sediments. In: Tucker M (ed.) Techniques in Sedimentology, 191- 228.

Hedley, R.H. 1958. Tube formation by *Pomatoceras triqueter* (Polychaeta). Journal of the Marine Biological Association. 37, 315-322.

Pillai, T.G. 2009. Description of New Serpulid Polychaetes from the Kimberleys of Australia and Discussion of Australian and Indo-West Pacific Species of *Spirobranchus* and Superficially Similar Taxa. Records of the Australian Museum. 61, 93-199.

Linnaeus, C. 1758. Systema Naturae, 10 ed. Vol. 1. L. Salvius, Holmiae 1758, 823 pp.

Philippi, A. 1844. Einige Bemerkungen über die Gattung *Serpula*, nebst Aufzählung der von mir im Mitteleer mit dem Their beobachteten Arten. Archiv für Naturgeschichte, Berlin. 10, 186-198.

Smith, A.M., Reidi, M.A., Winter, D.J. 2013. Temperate reefs in a changing ocean: skeletal carbonate mineralogy of serpulids. Marine Biology. 160, 2281-2294.

Taylor, P.D., Vinn, O., Kudryavtsev, A., Schopf, J.W. 2010. Raman spectroscopic study of the mineral composition of cirratulid tubes (Annelida, Polychaeta). Journal of Structural Biology. 171, 402-405.

Ten Hove, H.A., Kupriyanova, E.K. 2009. Taxonomy of Serpilidae (Annelida, Polychaeta): The state of affairs. Zootaxa 2036, Magnolia Press, Aukland, New Zealand, 126 pp.

Vinn, O. 2013. Occurrence, formation and function of organic sheets in the mineral tube structures of serpulidae (Polychaeta, Annelida). PLoS ONE. 8(10), e75330. doi:10.1371/journal.pone.0075330

Vinn, O., ten Hove, H.A., Mutvei, H., Kirsimae, K. 2008. Ultrastructure and mineral composition of serpulid tubes (Polychaeta, Annelida). Zoological Journal of the Linnean Society. 154, 633-650.

Vinn, O., ten Hove, H.A. 2011. Microstructure and formation of the calcareous operculum in *Pyrgopolan ctenactis* and *Spirobranchus giganteus* (Annelida, Serpulidae). Zoomorphology. 130, 181-188.

Vinn, O., Kirsimae, K., ten Hove, H.A. 2009. Tube ultrastructure of *Pomatoceros* americanus (Polychaeta, Serpulidae): implications for the tube formation of serpulids. Estonian Journal of Earth Sciences. 58, 148-152.

Vinn, O., Zaton, M. 2012. Inconsistencies in proposed annelid affinities of early biomineralized organism *Cloudina* (Ediacaran): structural and ontogenetic evidences. Carnets de Géologie. 2012/03, 39-47.

Weedon, M.J. 1994. Tube microstructure of Recent and Jurassic serpulid polychaetes and the question of the Palaeozoic ‘spirorbids. Acta Palaeontologica Polonica. 39, 1-15.

Zhang, F., Xu, H., Konishi, H., Roden, E. 2010. A relationship between d_{104} value and composition in the calcite-disordered dolomite solid-solution series. American Mineralogist. 95, 1650-1656.

Figure captions

Fig. 1. SEM images illustrating the general structure of *Pomatoceros triqueter*. (A) Vertical transverse section, illustrating 'triangular' cross-section. Displaying chevron layer (CL), pseudo-laminar layer (PLL), axial ridge (ar), alveoli (alv), and lumen (lum). (B) External surface of tube, around the aperture of a mature specimen. Displaying axial ridge (ar), peak (pk), and collar (cllr). (C), (D) Longitudinal sections through tube. Aperture towards the right. Displaying relationship between chevron layer (CL) and pseudo-laminar layer (PLL). Darker areas within the chevron layer represent organic membranes. In (C) note low angle of lamellae in pseudo-laminar layer that pass into chevron structure within the chevron layer. Within (D) the boundary between chevron layer and pseudo-laminar layer is discontinuous and unconformable. (E), (F) Typical shape of opercula, with conical, and cap shaped with tripartite horns respectively. (G) Tabulae from the distal end of tube. (H) Platey fabric of tabulae structure.

Fig. 2. Schematic longitudinal section through the tube wall of *Pomatoceros triqueter*, illustrating general distribution of fabrics and overall differentiated chevron structure. Key: Light grey = lamello-fibrillar fabric, dark grey = irregularly oriented prismatic fabric, white = spherulitic-prismatic fabric. PLL = pseudo-laminar layer, CL = chevron layer. Arrow indicates direction of tube construction. Alveoli not illustrated, but occur across the whole width of the chevron layer.

Fig. 3. SEM images of fabrics within *Pomatoceros triqueter*. (A) Lamello-fibrillar fabric, observed in longitudinal section, showing alternating direction of lath orientation between lamellae. (B) Irregularly oriented prismatic fabric showing chaotic irregular orientation of laths. **(**C), (D) Spherulitic-prismatic fabric, showing radiating structure and fine acicular sub-structure (C), and initiation along an organic membrane (Om) (D). (E) Alternating lamellae of lamello-fibrillar fabric (Lf) with organic membranes (Om), direction of growth towards bottom left. (F) Detail of organic membrane (Om) from (E), showing fibres and membranes. (G) Interface between spheroidal-prismatic (Sp) base, organic membrane (Om) and lozenge fabric (Lo). (H) Detail of lozenge fabric.

Fig. 4. SEM images of fabrics from the opercula of *Pomatoceros triqueter*. (A) Fibrous fabric, showing granular sub-structure. (B) Broken section showing radially developed fibrous texture (rd) and some developed parallel to surface (ps). Note internal surface (is). **(**C) External surface, between horns, displaying radially developed fibrous texture constrained within polygonal structures. (D) Polygonal arrangement on internal surface of opercula. Note low amplitude mounds. (E) Granlar texture, closely associated with fibrous texture. (F) Large spheroidal structures (viewed from external surface). Note the occurrence of diatoms (diat). (G) Sinuous hollow tubes developed just below the outer surface, near apex of opercula. (H) Detail of sinuous tubes, showing bladed and acicular crystals growing towards the centre of tube.

Tables

Table 1. Calcite d_{104} peak position from XRD, and calculated magnesium calcite content for eight samples of *Pomatoceros triqueter*. Arranged in terms of latitude, starting with the furthest north. Mol% $MgCO_3$ and Wt% $MgCO_3$ based upon d_{104} spacings, for various locations. Key: ‡ estimated based on Hardy & Tucker (1988, fig. 7.22), † Calculated using the method in Smith et al., 2013.

Location	Latitude	Calcite d_{104}	Mol% $MgCO_3$ ‡	Wt% $MgCO_3$ †
Rassay	57.3969°N	2.99, 3.01	15, 10	12.94, 8.55
Ballachulish	56.6755°N	2.99	15	12.94
Largs	55.7925°N	3.00, 3.00	13, 13	11.18, 11.18
Arran	55.5735°N	3.00, 3.00	13, 13	11.18, 11.18
Weymouth	50.6130°N	3.01	10	8.55

Figure
Click here to download high resolution image

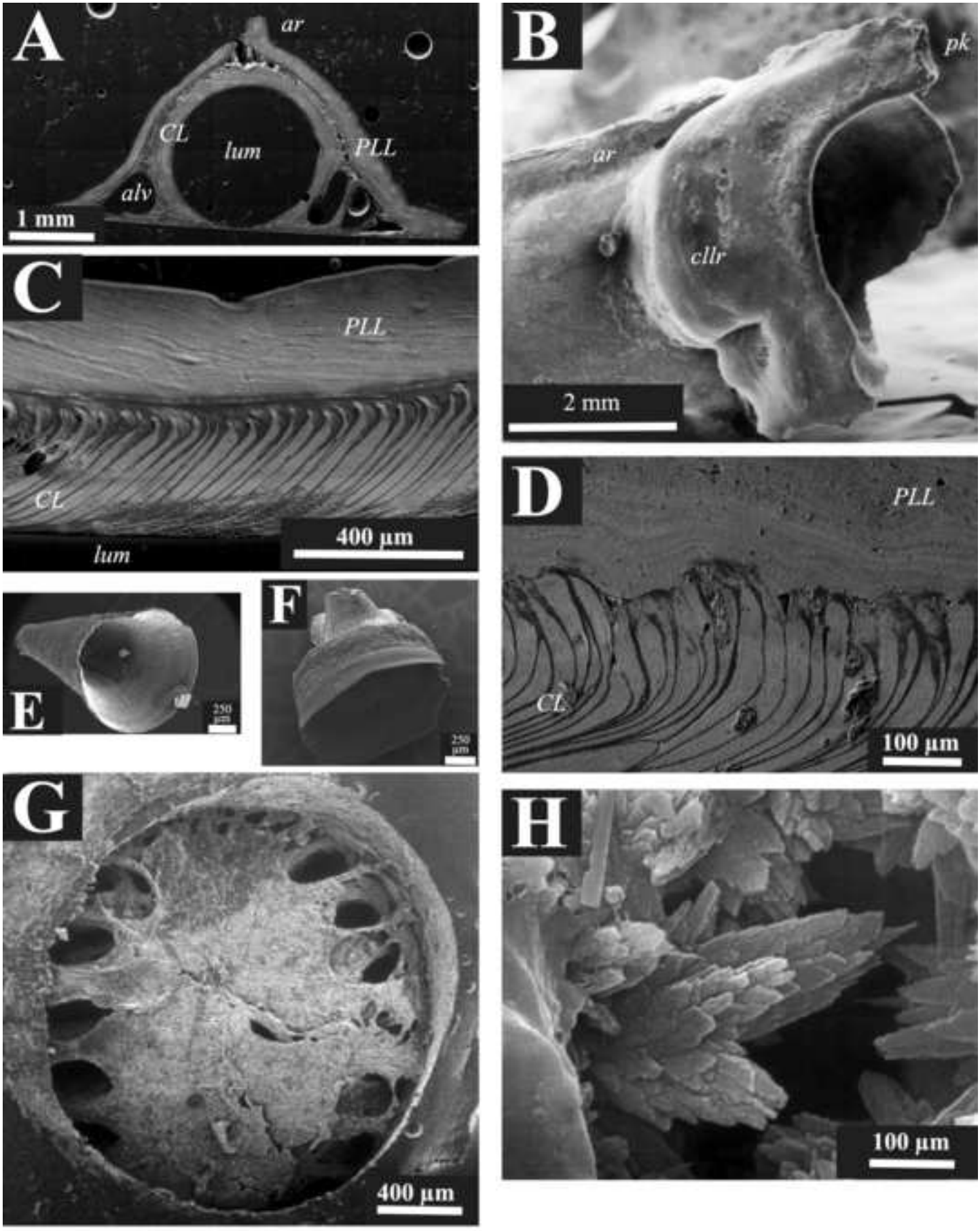

Figure

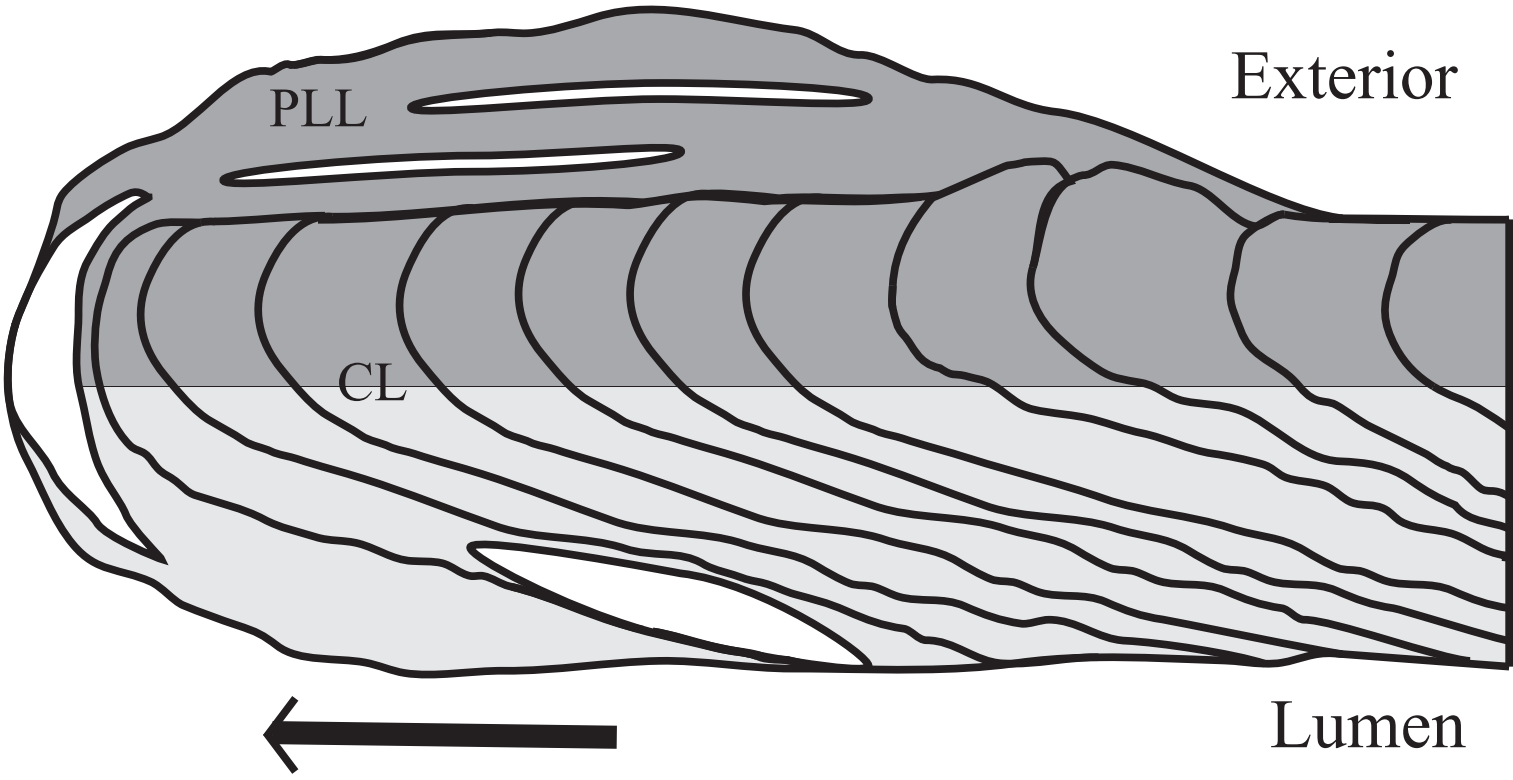

Figure

Click here to download high resolution image

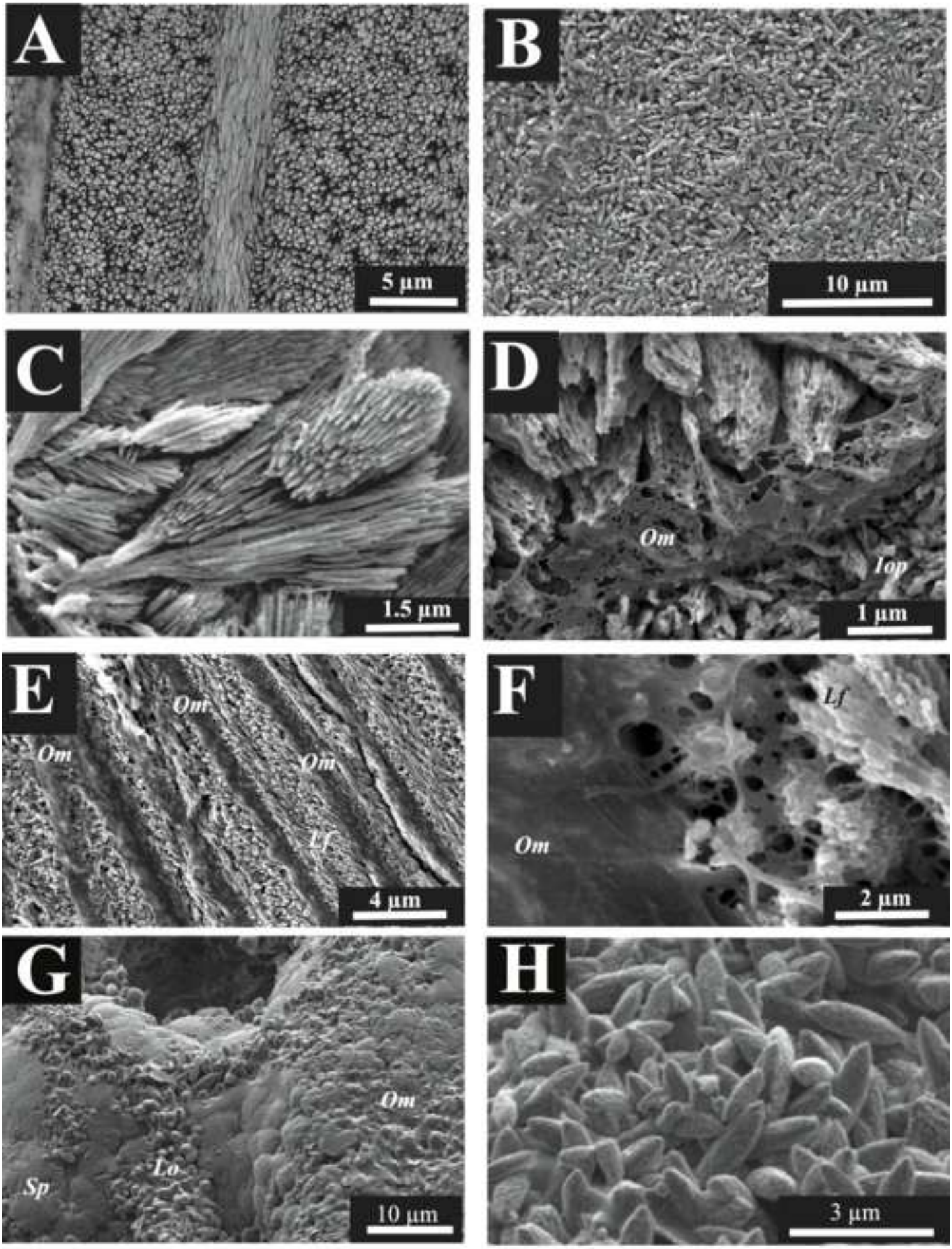

Figure
Click here to download high resolution image